

Two-boson field quantisation and flavour in q^+q^- mesons

H.P. Morsch¹

Institute for Nuclear Studies, PL-00681 Warsaw, Poland

Abstract

The flavour degree of freedom in non-charged $q\bar{q}$ mesons is discussed in a generalisation of quantum electrodynamics including scalar coupling of gauge bosons, which yields to an understanding of the confinement potential in mesons. The known “flavour states” σ , ω , Φ , J/Ψ and Υ can be described as fundamental states of the $q\bar{q}$ meson system, if a potential sum rule is applied, which is related to the structure of vacuum. This indicates a quantisation in fundamental two-boson fields, connected directly to the flavour degree of freedom.

In comparison with potential models additional states are predicted, which explain the large continuum of scalar mesons in the low mass spectrum and new states recently detected in the charm region.

PACS/ keywords: 11.15.-q, 12.40.-y, 14.40.Cs, 14.40.Gx/ Generalisation of quantum electrodynamics with massless elementary fermions (quantons, q) and scalar two-boson coupling. Confinement potential. Flavour degree of freedom of mesons described by fundamental q^+q^- states. Masses of σ , ω , Φ , J/Ψ and Υ .

The flavour degree of freedom has been observed in hadrons, but also in charged and neutral leptons, see e.g. ref. [1]. It is described in the Standard Model of particle physics by elementary fermions of different flavour quantum number. The fact that flavour is found in both strong and electroweak interactions could point to a supersymmetry between these fundamental forces, which should give rise to a variety of supersymmetric particles, which in spite of extensive searches have not been observed.

A very different interpretation of the flavour degree of freedom is obtained in an extension of quantum electrodynamics, in which the property of confinement of mesons as well as

¹postal address: Institut für Kernphysik, Forschungszentrum Jülich, D-52425 Jülich, Germany
E-mail: h.p.morsch@gmx.de

their masses are well described. This is based on a Lagrangian [2], which includes a scalar coupling of two vector bosons

$$\mathcal{L} = \frac{1}{\tilde{m}^2} \bar{\Psi} i\gamma_\mu D^\mu (D_\nu D^\nu) \Psi - \frac{1}{4} F_{\mu\nu} F^{\mu\nu} , \quad (1)$$

where Ψ is a massless elementary fermion (quanton, q) field, $D_\mu = \partial_\mu - ig_e A_\mu$ the covariant derivative with vector boson field A_μ and coupling g_e , and $F^{\mu\nu} = \partial^\mu A^\nu - \partial^\nu A^\mu$ the field strength tensor. Since our Lagrangian is an extension of quantum electrodynamics, the coupling g_e corresponds to a generalized charge coupling $g_e \geq e$ between charged quantons q^+ and q^- . By inserting the explicit form of D^μ and $D_\nu D^\nu$ in eq. (1), this leads to the following two contributions with 2- and 3-boson ($2g$ and $3g$) coupling, if Lorentz gauge $\partial_\mu A^\mu = 0$ and current conservation is applied

$$\mathcal{L}_{2g} = \frac{-ig_e^2}{\tilde{m}^2} \bar{\Psi} \gamma_\mu \partial^\mu (A_\nu A^\nu) \Psi \quad (2)$$

and

$$\mathcal{L}_{3g} = \frac{-g_e^3}{\tilde{m}^2} \bar{\Psi} \gamma_\mu A^\mu (A_\nu A^\nu) \Psi . \quad (3)$$

Requiring that $A_\nu A^\nu$ corresponds to a background field, \mathcal{L}_{2g} and \mathcal{L}_{3g} give rise to two first-order $q^+ q^-$ matrix elements

$$\mathcal{M}_{2g} = \frac{-\alpha_e^2}{\tilde{m}^3} \bar{\psi}(\tilde{p}') \gamma_\mu \partial^\mu \partial^\rho w(q) g_{\mu\rho} \gamma_\rho \psi(\tilde{p}) \quad (4)$$

and

$$\mathcal{M}_{3g} = \frac{-\alpha_e^3}{\tilde{m}} \bar{\psi}(\tilde{p}') \gamma_\mu w(q) \frac{g_{\mu\rho} f(p_i)}{p_i^2} w(q) \gamma_\rho \psi(\tilde{p}) , \quad (5)$$

in which $\alpha_e = g_e^2/4\pi$ and $\psi(\tilde{p})$ is a two-fermion wave function $\psi(\tilde{p}) = \frac{1}{\tilde{m}^3} \Psi(p) \Psi(k)$. The momenta have to respect the condition $\tilde{p}' - \tilde{p} = q + p_i = P$. Further, $w(q)$ is the two-boson momentum distribution and $f(p_i)$ the probability to combine q and P to $-p_i$. Since $f(p_i) \rightarrow 0$ for $\Delta p \rightarrow 0$ and ∞ , there are no divergencies in \mathcal{M}_3 .

By contracting the γ matrices by $\gamma_\mu \gamma_\rho + \gamma_\rho \gamma_\mu = 2g_{\mu\rho}$, reducing eqs. (4) and (5) to three dimensions, and making a transformation to r -space (details are given in ref. [2]), the following two potentials are obtained, which are given in spherical coordinates by

$$V_{2g}(r) = \frac{\alpha_e^2 \hbar^2 \tilde{E}^2}{\tilde{m}^3} \left(\frac{d^2 w(r)}{dr^2} + \frac{2}{r} \frac{dw(r)}{dr} \right) \frac{1}{w(r)} , \quad (6)$$

where $\tilde{E} = \langle E^2 \rangle^{1/2}$ is the mean energy of scalar states of the system, and

$$V_{3g}^{(1^-)}(r) = \frac{\hbar}{\tilde{m}} \int dr' \rho(r') V_g(r - r') , \quad (7)$$

in which $w(r)$ and $\rho(r)$ are two-boson wave function and density (with dimension $f m^{-2}$), respectively, related by $\rho(r) = w^2(r)$. Further, $V_g(r - r')$ is an effective boson-exchange interaction $V_g(r) = -\alpha_e^3 \hbar \frac{f(r)}{r}$. Since the quanton-antiquanton parity is negative, the potential (7) corresponds to a binding potential for vector states (with $J^\pi = 1^-$). For scalar states angular momentum $L=1$ is needed, requiring a p-wave density, which is related to $\rho(r)$ by

$$\rho^p(\vec{r}) = \rho^p(r) Y_{1,m}(\theta, \Phi) = (1 + \beta R d/dr) \rho(r) Y_{1,m}(\theta, \Phi) . \quad (8)$$

βR is determined from the condition $\langle r_{\rho^p} \rangle = \int d\tau r \rho^p(r) = 0$ (elimination of spurious motion). This yields a boson-exchange potential given by

$$V_{3g}^{(0^+)}(r) = \frac{\hbar}{\tilde{m}} \int d\vec{r}' \rho^p(\vec{r}') Y_{1,m}(\theta', \Phi') V_g(\vec{r} - \vec{r}') = 4\pi \frac{\hbar}{\tilde{m}} \int dr' \rho^p(r') V_g(r - r') . \quad (9)$$

We require a matching of $V_{3g}^{(0^+)}(r)$ and $\rho(r)$

$$V_{3g}^{(0^+)}(r) = c_{pot} \rho(r) , \quad (10)$$

where c_{pot} is an arbitrary proportionality factor. Eq. (10) is a consequence of the fact that $V_g(r)$ should be finite for all values of r . This can be achieved by using a form

$$V_g(r) = f_{as}(r) (-\alpha_e^3 \hbar / r) e^{-cr} \quad (11)$$

with $f_{as}(r) = (e^{(ar)^\sigma} - 1) / (e^{(ar)^\sigma} + 1)$, where the parameters c , a and σ are determined from the condition (10).

Self-consistent two-boson densities are obtained assuming a form

$$\rho(r) = \rho_o [\exp\{-(r/b)^\kappa\}]^2 \quad \text{with } \kappa \simeq 1.5 . \quad (12)$$

The matching condition (10) is rather strict (see fig. 1) and determines quite well the parameter κ of $\rho(r)$: using a pure exponential form ($\kappa=1$) a very steep rise of $\rho(r)$ is obtained for $r \rightarrow 0$, but an almost negligible and flat boson-exchange potential, which cannot satisfy eq. (10). Also for a Gaussian form ($\kappa=2$) no consistency is obtained, the

deduced potential falls off more rapidly towards larger radii than the density $\rho(r)$. The agreement between $\langle r_\rho^2 \rangle$ and $\langle r_{V_{3g}}^2(r) \rangle$ cannot be enforced by using a different parametrisation for $f_{as}(r)$. Only by a density with $\kappa \simeq 1.5$ a satisfactory solution is obtained.

For our solution (12) it is important to verify that $V_g(r)$ is quite similar in shape to $\rho^p(r)$ required from the modification of the boson-exchange propagator. This is indeed the case, as shown in the upper part of fig. 2, which displays solution 4 in the tables. Further, the low radius cut-off function $f_{as}(r)$ is shown by the dashed line, which falls off to zero for $r \rightarrow 0$. A transformation to momentum (Q) space leads to $f_{as}(Q) \rightarrow 0$ for $Q \rightarrow \infty$. Interestingly, this decrease of $f_{as}(Q)$ for large momenta is quite similar to the behaviour of quantum chromodynamics, a slowly falling coupling strength $\alpha(Q)$ related to the property of asymptotic freedom [3].

In the two lower parts of fig. 2 the resulting two-boson density and the boson-exchange potential (9) are shown in r - and Q -space² for solution 4 in the tables, both in very good agreement. In the Fourier transformation to Q -space the process $gg \rightarrow q\bar{q}$ is elastic and consequently the created $q\bar{q}$ -pair has no mass. However, if we take a finite mass of the created fermions of 1.4 GeV (such a mass has been assumed for a comparable system in potential models [4]), a boson-exchange potential is obtained (given by the dashed line in the lower part of fig. 2), which cannot be consistent with the density $\rho(r)$. Thus, our solutions require **massless** fermions. This allows to relate the generated system to the absolute vacuum of fluctuating boson fields with energy $E_{vac} = 0$.

The mass of the system is given by

$$M_n^m = -E_{3g}^m + E_{2g}^n, \quad (13)$$

where E_{3g}^m and E_{2g}^n are binding energies in $V_{3g}(r)$ and $V_{2g}(r)$, respectively, calculated by using a mass parameter $\tilde{m} = 1/4 \tilde{M} = 1/4 \langle Q_\rho^2 \rangle^{1/2}$, where \tilde{M} is the average mass generated, and \tilde{E} given in table 2. The coupling constant α_e is determined by the matching of the binding energies to the mass, see eq. (13). The boson-exchange potential is attractive and has negative binding energies, with the strongest bound state having the largest mass and excited states having smaller masses. These energies do not increase the mean energy E_{vac} of the vacuum: writing the energy-momentum relation

²In Q -space multiplied by Q^2 .

Table 1: Deduced masses (in GeV) of scalar and vector q^+q^- states in comparison with known 0^{++} and 1^{--} mesons [1] (for $V_{3g}(r)$ only the lowest bound state is given).

Solution	(meson)	M_1^1	M_2^1	M_3^1	M_1^{exp}	M_2^{exp}	M_3^{exp}
1	scalar σ	0.55	1.28	1.88	0.60 ± 0.2	1.35 ± 0.2	
2	scalar f_o	1.38	2.25	2.9	1.35 ± 0.2		
	vector ω	0.78	1.65	2.3	0.78	1.65 ± 0.02	
3	scalar f_o	2.68	3.34	3.9	—		
	vector Φ	1.02	1.68	2.23	1.02	1.68 ± 0.02	
4	scalar not seen	11.7	12.3	12.8	—		
	vector J/Ψ	3.10	3.69	4.16	3.097	3.686	(4.160)
5	scalar not seen	40.5	41.0	41.4	—		
	vector Υ	9.46	9.98	10.38	9.46	10.023	10.355

$E_{vac} = 0 = \sqrt{\langle Q_\rho^2 \rangle} + E_{3g}$, this relation is conserved, if E_{3g} is compensated by the root mean square momentum of the deduced density $\langle Q_\rho^2 \rangle^{1/2}$.

Differently, the binding energy in the self-induced two-boson potential (6), which does not appear in normal gauge theory applications (see ref. [1]), is positive and corresponds to a real mass generation by increasing the total energy by E_{2g} . Therefore, this potential allows a creation of stationary $(q\bar{q})^n$ states out of the absolute vacuum of fluctuating boson fields, if two rapidly fluctuating boson fields overlap and cause a quantum fluctuation with energy E_{2g} . The two-boson potential $V_{2g}(r)$ (with density parameters from solution 4 in the tables) is compared to the confinement potential from lattice gauge calculations [5] in the upper part of fig. 3, which shows good agreement. The corresponding potentials obtained from the other solutions are very similar, if a small decrease of κ is assumed for solutions of stronger binding (as given in table 2).

We have seen in fig. 1 that the functional shape of the two-boson density (12) (given by the parameter κ) is quite well determined. In contrary, we find that the slope parameter b (which governs the radial extent $\langle r_\rho^2 \rangle$) is not constrained by the different conditions applied. This allows a continuum of solutions with different radius. However, on the fundamental level of overlapping boson fields quantum effects are inherent and should give

Table 2: Parameters and deduced values of $\langle Q_\rho^2 \rangle^{1/2}$, \tilde{E} in GeV and $\langle r^2 \rangle$ in fm^2 for the different solutions. b is given in fm , c and a in fm^{-1} . The values of $\langle r^2 \rangle_{exp}$ are taken from ref. [6].

Sol.	κ	b	α_e	c	a	σ	$\langle Q_\rho^2 \rangle^{1/2}$	\tilde{E}	$\langle r_\rho^2 \rangle$	$\langle r^2 \rangle_{exp}$
1	1.50	0.77	0.26	2.4	6.4	0.86	0.59	0.9	0.65	–
2	1.46	0.534	0.385	3.3	12.0	0.86	0.81	1.0	0.33	0.33
3	1.44	0.327	0.44	5.35	16.4	0.85	1.44	1.3	0.13	0.21
4	1.40	0.125	0.58	13.6	50.7	0.83	3.50	1.6	0.02	0.04
5	1.37	0.042	0.635	46.0	132.6	0.82	10.46	2.3	0.002	–

rise to discrete solutions. Such a (new) quantisation can only arise from an additional constraint originating from the structure of the vacuum. This may be formulated in the form of a vacuum potential sum rule.

We assume the existence of a global boson-exchange interaction in the vacuum $V_{vac}(r)$, which has a radial dependence similar to the boson-exchange interaction (11) discussed above, but with an additional $1/r$ fall-off, which leads to $V_{vac}(r) \sim 1/r^2$. Further, we require that the different potentials $V_{3g}^i(r)$ (where i are discrete solutions) sum up to $V_{vac}(r)$

$$\sum_i V_{3g}^i(r) = V_{vac}(r) = \tilde{f}_{as}(r)(-\tilde{\alpha}_e^3 \hbar r_o/r^2) e^{-\tilde{c}r}, \quad (14)$$

where $\tilde{f}_{as}(r)$ and $e^{-\tilde{c}r}$ are cut-off functions as in eq. (11). Actually, we expect that the cut-off functions should be close to those for the state with the lowest mass. Interestingly, the radial forms of $V_g(r)$ and $V_{vac}(r)$ are the only two forms, which lead to equally simple forms in Q-space: $1/r \rightarrow 1/Q^2$ and $1/r^2 \rightarrow 1/Q$. This supports our assumption.

If we assume that the new quantisation is related to the flavour degree of freedom, the different “flavour states” of mesons ω , Φ , J/Ψ , and Υ should correspond to eigenstates of the sum rule (14). Indeed, we find that the sum of the boson-exchange potentials with g.s. masses of 0.78, 1.02, 3.1 and 9.4 add up to a potential, which is in reasonable agreement with the sum (14). However, the needed cut-off parameters a , σ , and c correspond to those for the $\sigma(600)$ solution (see ref. [2]). This can be regarded as strong evidence for the $\sigma(600)$ being to the lowest flavour state. By inclusion of this solution also, a good agreement

with the sum rule (14) is obtained. This is shown in the lower part of fig 3, where the different potentials are given by dashed and dot-dashed lines with their sum given by the solid line. The resulting masses of scalar and vector states together with their excited states in $V_{2g}(r)$ are given in table 1, which are in good agreement with experiment for the known states. The corresponding density parameters are given in table 2 with mean square radii in reasonable agreement with the meson radii extracted from experimental data (see ref. [6]). It is evident that in this multi-parameter fit there are ambiguities, which can be reduced only by detailed studies of the contributions of the different states to the average mass \tilde{E} and its relation to $\langle Q_\rho^2 \rangle^{1/2}$. However, the reasonable account of the experimental masses and the quantitative fit of the sum rule (14) in fig. 3 indicates that our results are quite correct.

As compared to potential models using finite fermion (quark) masses (see e.g. ref. [4]), we obtain significantly more states, bound states in $V_{2g}(r)$ and in $V_{3g}(r)$. The solutions in table 1 correspond only to the 1s level in $V_{3g}(r)$, in addition there are Ns levels with N=2, 3, ... Most of these states, however, have a relatively small mass far below 3 GeV. As the boson-exchange potential is Coulomb like, it creates a continuum of Ns levels with masses, which range down to the threshold region. This is consistent with the average energy \tilde{E} of scalar excitations in table 2, which increases much less for heavier systems as compared to the energy of the 1s-state. These low energy states give rise to large phase shifts at low energies, in particular large scalar phase shifts.

Concerning masses above 3 GeV, solution 5 yields additional scalar 2s and 3s states at masses of about 12 and 8.8 GeV, respectively, whereas an extra vector 2s state is obtained (between the most likely $\Psi(3s)$ and $\Psi(4s)$ states at 4.160 GeV and 4.415 GeV) at a mass of about 4.2 GeV. This state may be identified with the recently discovered X(4260), see ref. [1]. Corresponding excited states in the confinement potential (6) should be found at masses of 4.9, 5.3 and 5.5 GeV with uncertainties of 0.2-0.3 GeV.

In summary, the present model based on an extension of electrodynamics leads to a good understanding of the confinement and the masses of fundamental $q\bar{q}$ mesons. The flavour degree of freedom is described by stationary states of different radial extent, whose potentials exhaust a vacuum potential sum rule. In a forthcoming paper a similar description

will be discussed for neutrinos, which supports our conclusion that the flavour degree of freedom is related to the structure of overlapping boson fields in the vacuum.

Fruitful discussions and valuable comments from P. Decowski, M. Dillig (deceased), B. Loiseau and P. Zupranski among many other colleagues are appreciated.

References

- [1] Review of particle properties, C. Amsler et al., Phys. Lett B 667, 1 (2008); <http://pdg.lbl.gov/> and refs. therein
- [2] H.P. Morsch, “Inclusion of scalar boson coupling in fundamental gauge theory Lagrangians”, to be published
- [3] D.J. Gross and F. Wilczek, Phys. Rev. Lett. 30, 1343 (1973); H.D. Politzer, Phys. Rev. Lett. 30, 1346 (1973) (2005) and refs. therein
- [4] R. Barbieri, R. Kögerler, Z. Kunszt, and R. Gatto, Nucl. Phys. B 105, 125 (1976); E. Eichten, K.Gottfried, T. Kinoshita, K.D. Lane, and T.M. Yan, Phys. Rev. D 17, 3090 (1978); S. Godfrey and N. Isgur, Phys. Rev. D 32, 189 (1985); D. Ebert, R.N. Faustov, and V.O. Galkin, Phys. Rev. D 67, 014027 (2003); and refs. therein
- [5] G.S. Bali, K. Schilling, and A. Wachter, Phys. Rev. D 56, 2566 (1997); G.S. Bali, B. Bolder, N. Eicker, T. Lippert, B. Orth, K. Schilling, and T. Struckmann, Phys. Rev. D 62, 054503 (2000)
- [6] H.P. Morsch, Z. Phys. A 350, 61 (1994)
- [7] M. Ablikim, et al., hep-ex/0406038 (2004); see also D.V. Bugg, hep-ex/0510014 (2005) and refs. therein 16, 229 (2003)

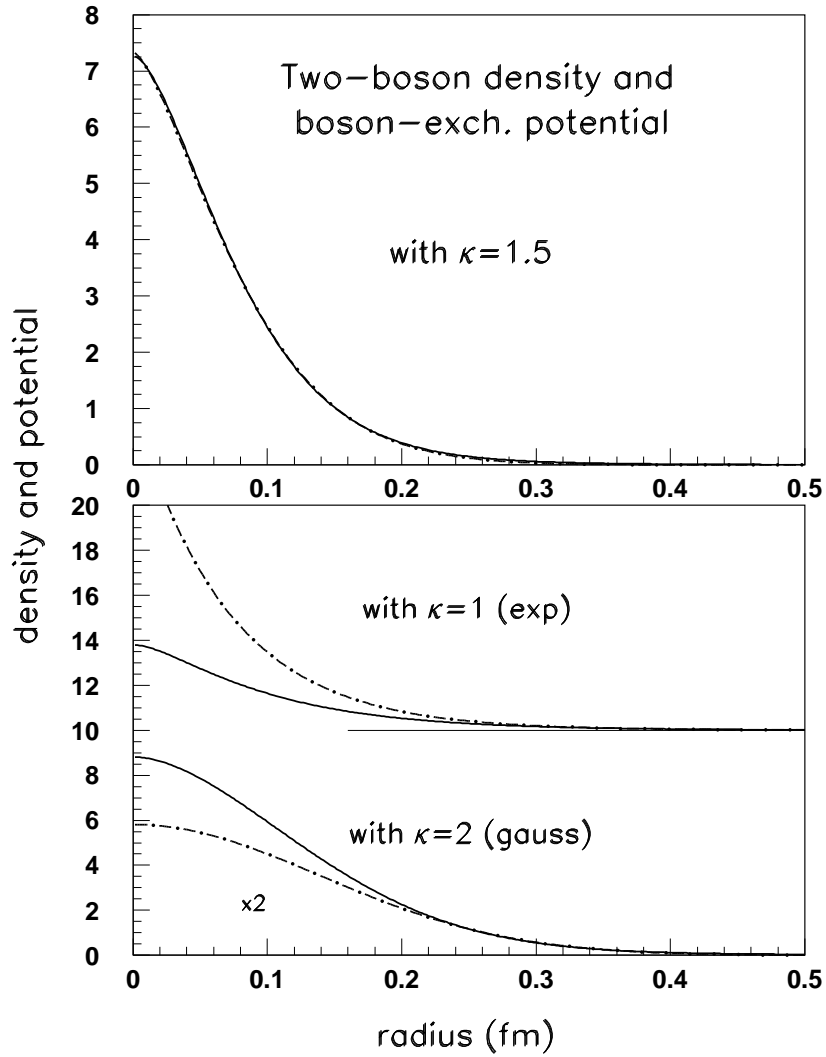


Figure 1: Comparison of two-boson density for $\langle r_\rho^2 \rangle = 0.2 \text{ fm}^2$ (dot-dashed lines) and boson-exchange potential $|V_{3g}(r)/c_{pot}|$ (solid lines) for $\kappa=1.5, 1$ and 2 , respectively.

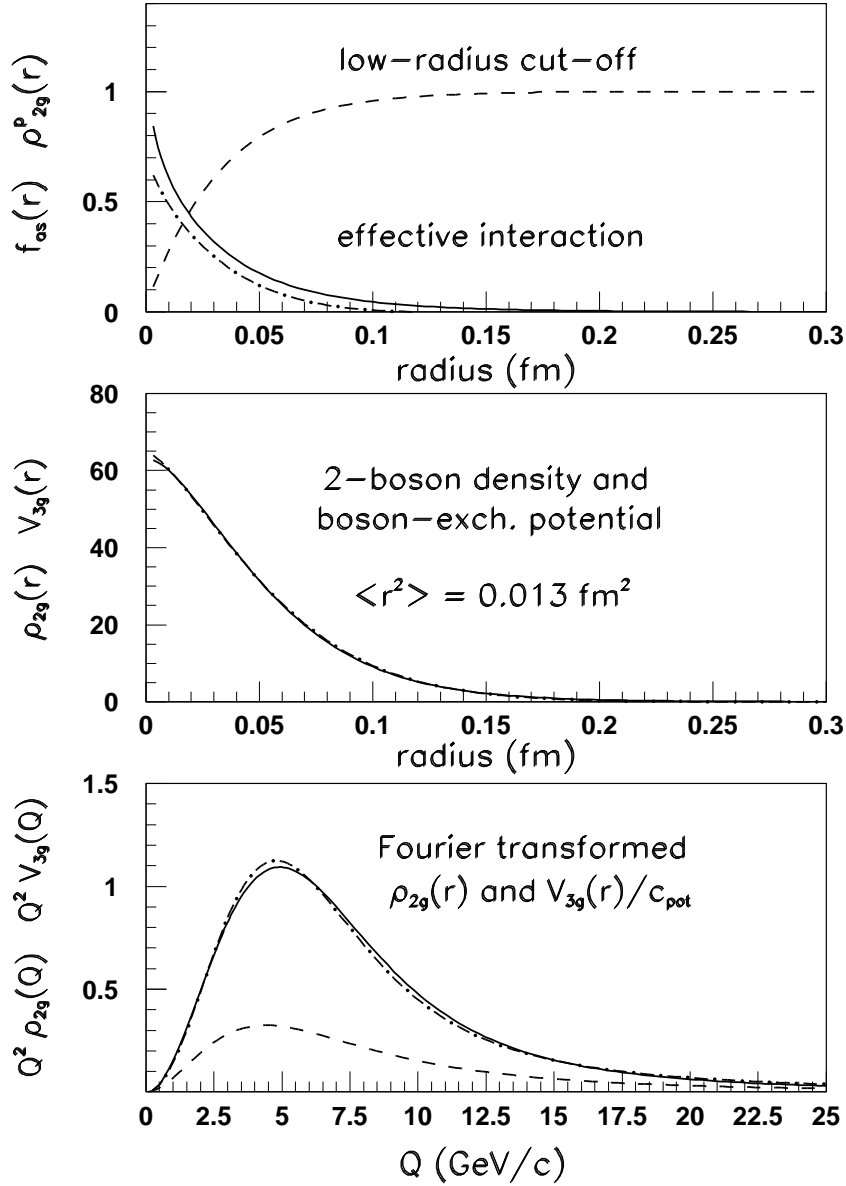


Figure 2: Self-consistent solution with $\langle r_\rho^2 \rangle = 0.013 \text{ fm}^2$. Upper part: Low radius cut-off function $f_{as}(r)$, shape of interaction (11) and $\rho^p(r)$ given by dashed, solid and dot-dashed lines, respectively. Lower two parts: Two-boson density and boson-exchange potential $|V_{3g}/c_{pot}|$ in r- and Q-space, for the latter multiplied by Q^2 , given by the overlapping dot-dashed and solid lines, respectively. The dashed line in the lower part corresponds to a calculation assuming fermion masses of 1.4 GeV.

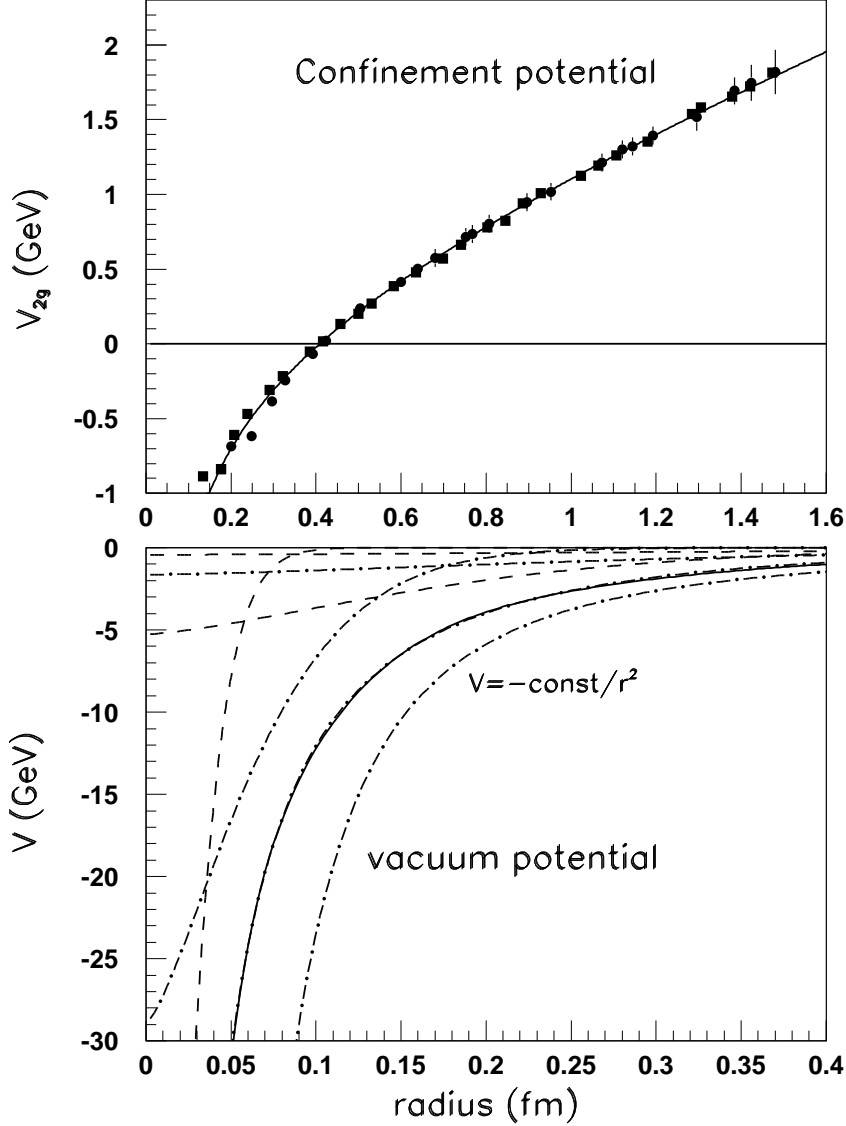


Figure 3: Upper part: Deduced confinement potential $V_{2g}(r)$ (6) taken from solution 4 (solid line) in comparison with lattice gauge calculations [5] (solid points) . Lower part: Boson-exchange potentials for the different solutions in the tables (given by dot-dashed and dashed lines) and sum given by solid line. This is compared to the vacuum sum rule (14) given by the dot-dashed line overlapping with the solid line. A pure potential $V = -\text{const}/r^2$ is shown also by the lower dot-dashed line.